Supplement of Geosci. Model Dev., 19, 11243–11263, 2026
https://doi.org/10.5194/gmd-19-11243-2026-supplement
© Author(s) 2026. CC BY 4.0 License.



Geoscientific Model Development Open Access EGU

Supplement of

GEOS-Chem-hyd: enabling source-oriented sensitivity analysis with GEOS-Chem

Samuel O. Akinjole et al.

Correspondence to: Shannon L. Capps (shannon.capps@drexel.edu)

The copyright of individual parts of the supplement might differ from the article licence.

S1 HEMCO Sensitivity Evaluation

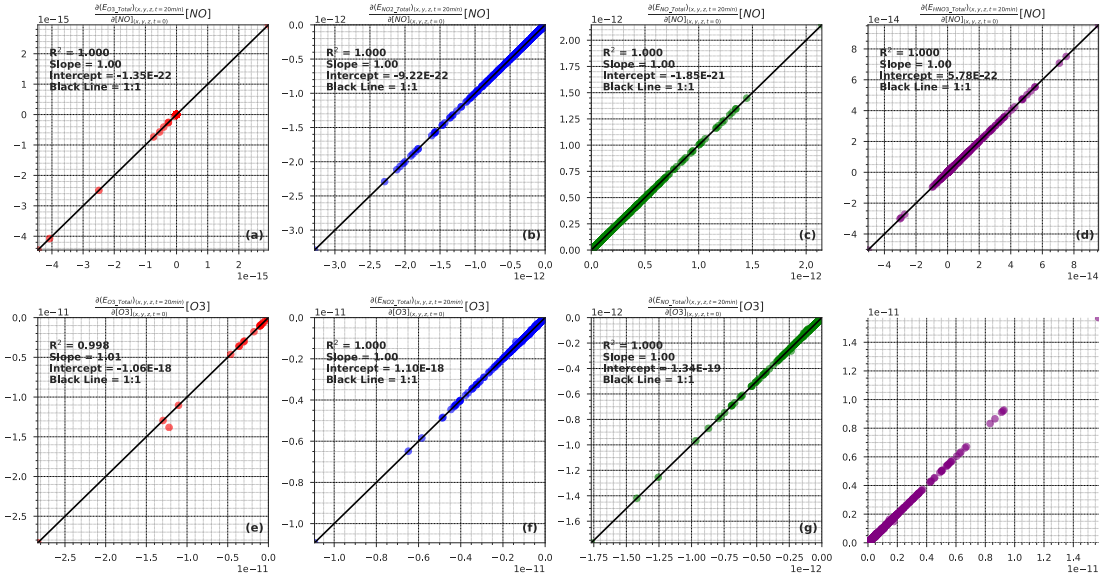

Figure S1: Comparison of the first-order semi-normalized sensitivities of emissions of species at the end of an emission timestep with respect to perturbation in NO concentration (*a*-*d*) and O_3 concentration (*e*-*h*) for GEOS-Chem-hyd (*y*-axis) and the central finite difference method (*x*-axis) at 1 % perturbation.

For the second-order sensitivities, only the species with observed non-linear relationships are shown below.

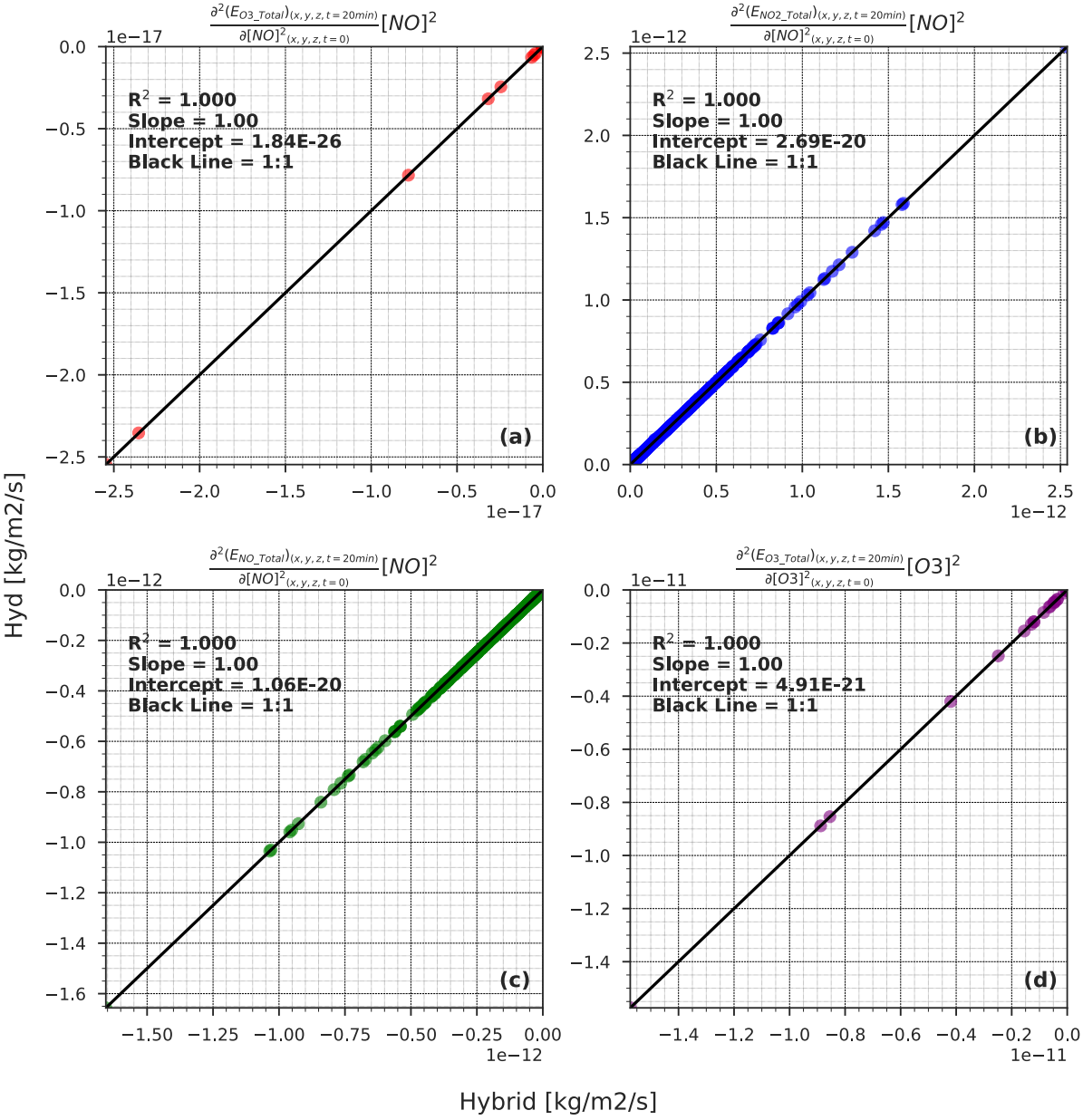

Figure S2. Comparison of the second-order semi-normalized sensitivities of emissions of species at the end of an emission timestep with respect to perturbation in NO concentration (*a-c*) at 1 % perturbation and O_3 concentration (*d*) at 0.01 % perturbation for GEOS-Chem-hyd (y-axis) and the hybrid method (x-axis).

S2 ISORROPIA-hyd Implementation

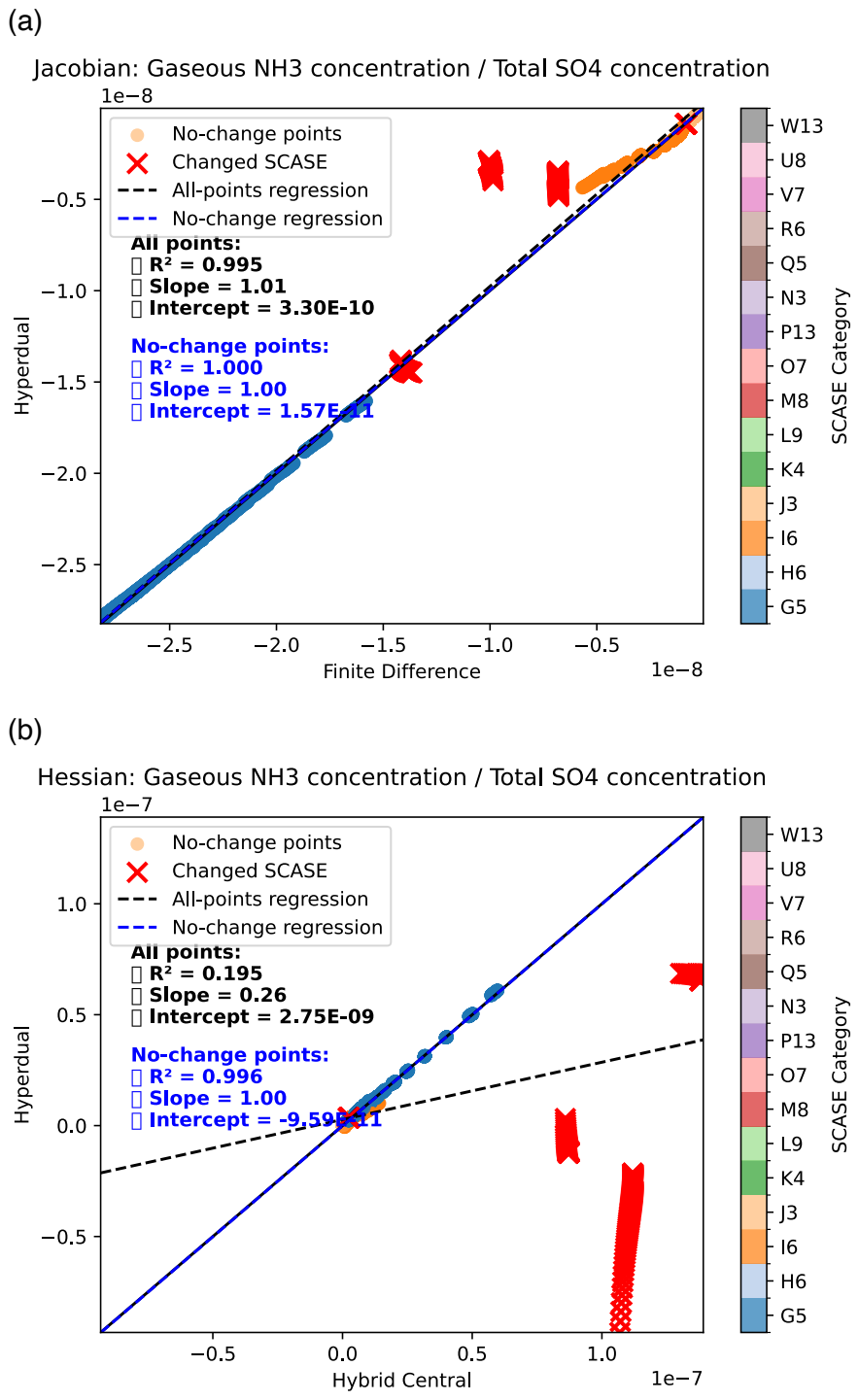

Figure S3. Comparison of the first-order (a) and second-order (b) hyperdual results to the central finite difference (a) and hybrid-hyd finite difference (b) results using standalone ISORROPIA II at 5 % perturbation. Tests were conducted at 297 K and 77 % RH, with NH4 and NO3 ranging from 1.0d-9 to 1.0d-7 mol/m^3. The input conditions for TNA, TSO4, TNH3, TNO3, TCL were fixed at 4.712d-9, 1.338d-8, 5.03d-8, 1.101d-8, and 1.35d-8 mol/m^3 respectively. X points represent scenarios in which case changes occur between the two perturbed runs when calculating the finite-difference sensitivities.

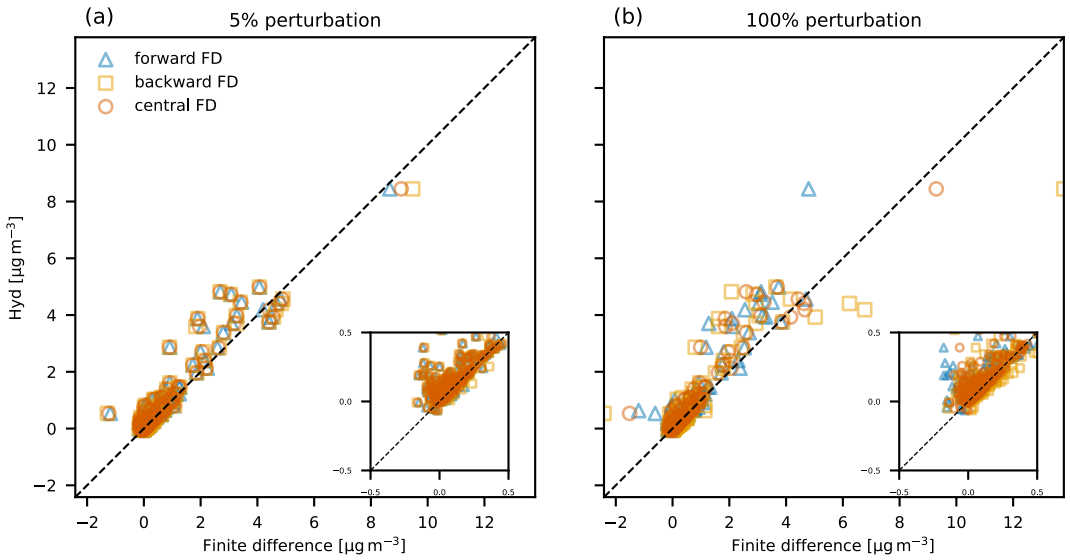

Figure S4. Comparison of first-order semi-normalized sensitivities of the time-averaged, ground layer $PM_{2.5}$ concentrations with respect to domain-wide, persistent perturbation of NO_x throughout the 24-hour episode using the hyperdual step method (Hyd) and forward, central, and backward FD methods with a 5 % (a) and 100 % (b) perturbation in each direction.

Table S1. Summary of modifications to ISORROPIA II for stable hyperdual number-based sensitivity analysis. The content of this table was generated with Claude by evaluating the base and augmented repositories; then, the table was checked by the authors.

Changes are grouped by type; the base implementation is GEOS-Chem v14.0.0-rc.3 ISORROPIA II. Sulfate-poor denotes ($[NH_4^+]$+[Na])/[SO_4] > 2 and sodium-poor [Na]/[SO_4] < 2; routine-level code detail is in the archived source.

Category	What was changed	Why it was needed
1. Hyperdual variable types	All aerosol concentration, ion, solid-phase and partitioning variables (~131 routines) converted from real to hyperdual; temperature and relative humidity stay real.	Sensitivity information travels only through variables that carry derivative components; T and RH are not perturbed here.
2. Numerically stable quadratic formula	Quadratic roots rewritten in the stable form of Press et al. (2007), also used in HETP (Miller et al., 2024). Negative discriminants are clipped to zero.	In the textbook form, b much larger than a and c makes $-b + \sqrt{(b^2 - 4ac)}$ a difference of nearly equal numbers. The lost digits barely shift the concentration but corrupt its derivative.
3. Tolerances and thresholds	"Is the input zero?" tests rescaled by the number of species summed (8×TINY for an eight-term sum), plus a new pH routine (CALCPH_g) using the toleranced square root of Category 10.	Eight individually negligible inputs can sum to more than the single-species threshold, so invalid air masses can be classified as significant.
4. Real-valued activity coefficients	Activity coefficients and ionic strength computed from the real part of molality and water content only. Fortran statement functions rewritten as module functions.	Differentiating the iterative Bromley activity-coefficient loop amplified sensitivities non-physically. Statement functions cannot be type-checked under implicit none.
5. Precision and type conversions	INT() replaced by INT_HDUAL(), which takes the real part before converting; integer-to-real conversions forced to double precision.	Fortran intrinsics do not accept hyperdual arguments, and a single-precision bisection step size would degrade the derivative it carries.
6. Gas-phase concentration floors	Lower bound on gas-phase HNO_3 and HCl lowered from TINY (10^{-20}) to zero, following HETP: $\mathrm{GHNO_3} = \max(\mathrm{W_4} - \mathrm{MOLAL_7}, \mathrm{TINY})$ $\rightarrow \mathrm{GHNO_3} = \max(\mathrm{W_4} - \mathrm{MOLAL_7}, 0)$ Aqueous NH_4^+ likewise floored at zero.	An artificial floor is invisible in the concentration but puts a kink at the zero boundary that appears as a discontinuous derivative. Gas-phase concentrations genuinely can be zero.
7. Real-valued bisection	Real-part-only copies (_no_sens) of the residual functions used inside the bisection search for G5 (sulphate-poor, sodium-poor) and H6 (sulphate-poor, sodium-rich).	Bisection needs only the sign of the residual; carrying hyperdual arithmetic through the search is wasteful, and the jumping midpoint shifts the derivatives it returns.
8. Tangent-linear (_D) routines	Companion routines generated by source transformation with Tapenade (Hascoet and Pascual, 2013) and adapted to hyperdual arithmetic, returning the slope of the residual alongside its value.	The Newton polish in Category 9 requires that slope. Tabulated activity coefficients are not differentiable, so their tangents are zeroed while the mixing rule downstream is still differentiated.
9. Newton–Raphson polish of the bisected root	Two Newton steps in full hyperdual arithmetic appended once bisection converges in G5 and H6: $X \leftarrow X - F(X)/F'(X)$ Activity coefficients are re-initialised before each evaluation.	Bisection returns a root with the right value but no derivative content. Each step transfers the implicit-function sensitivity $\partial\psi_6/\partial p = -(\partial F/\partial p) \,/\, (\partial F/\partial\psi_6)$ onto the root: the first restores first order exactly, the second the remaining second-order term.
10. Toleranced square root	In the G5 path only, √ replaced by sqrt_tol, which floors the argument at 10^{-17} when forming the derivative while leaving the real value exact.	The slope of the square root diverges as the discriminant collapses, $\mathrm{d}(\sqrt{q})/\mathrm{d}q = 1/(2\sqrt{q}) \rightarrow \infty \text{ as } q \rightarrow 0$ so pH and nitrate partitioning stay well behaved while their derivatives blow up. As tested, only necessary in G5.
11. Guards and per-cell diagnostics	A Newton step is rejected if it leaves the bracket found by bisection, and cells whose discriminant collapses below 10^{-18} are flagged. Both are tallied and mapped through History.	Affected cells are left unchanged rather than returning a corrupted sensitivity, and the fraction discarded can be reported rather than assumed negligible.

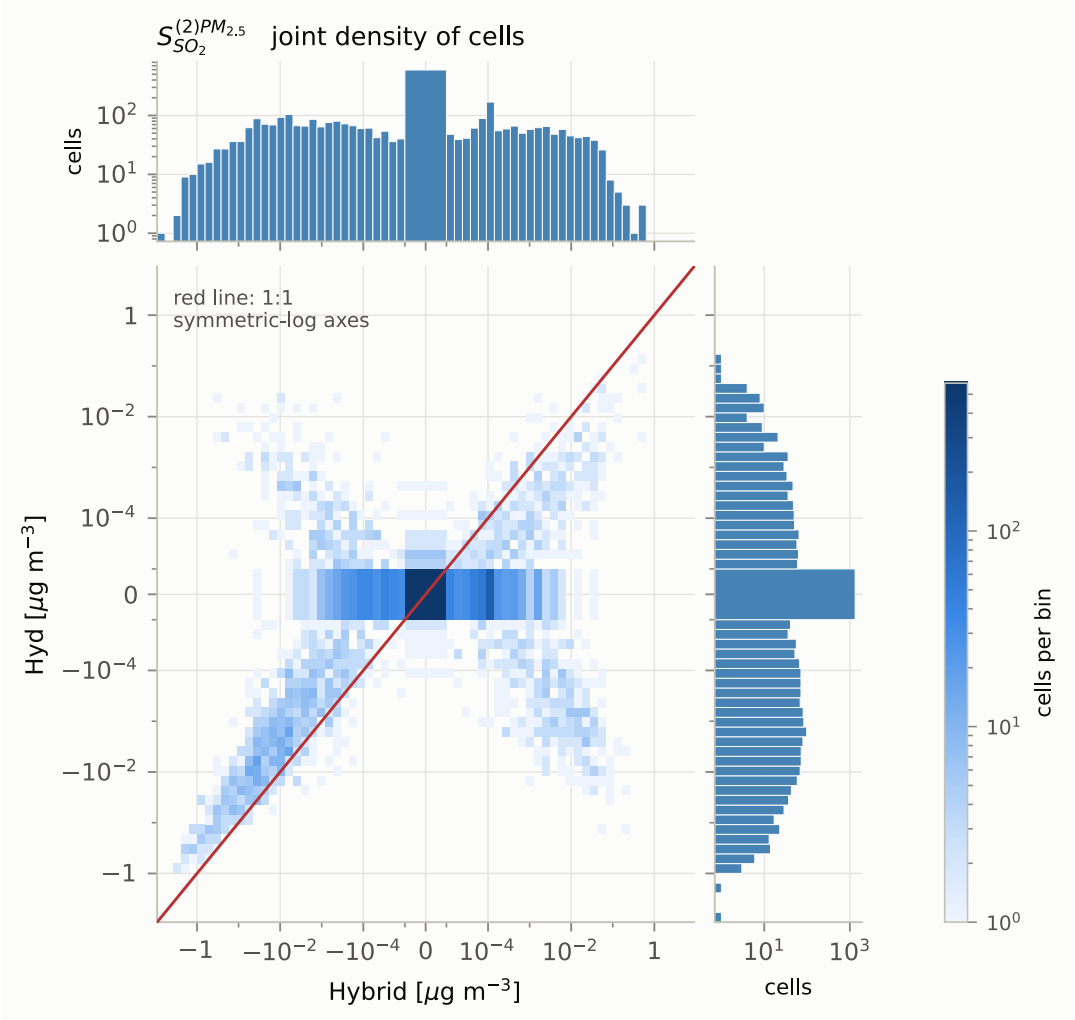

Figure S5. Joint heatmap and marginal distributions of second-order semi-normalized sensitivities of the time-averaged, ground layer $PM_{2.5}$ concentrations with respect to domain-wide, persistent perturbation of SO_2 emissions throughout the 24-hour episode, using the hyperdual step method (Hyd) and the hybrid hyperdual-finite difference method (Hybrid) with a 5 % perturbation in each direction. By cell count, 52.5 % of the hybrid values and 63.8 % of the hyperdual values are negative: the hyperdual values are negative more often but are clustered near zero, whereas in the hybrid it is the large-magnitude values that are predominantly negative.

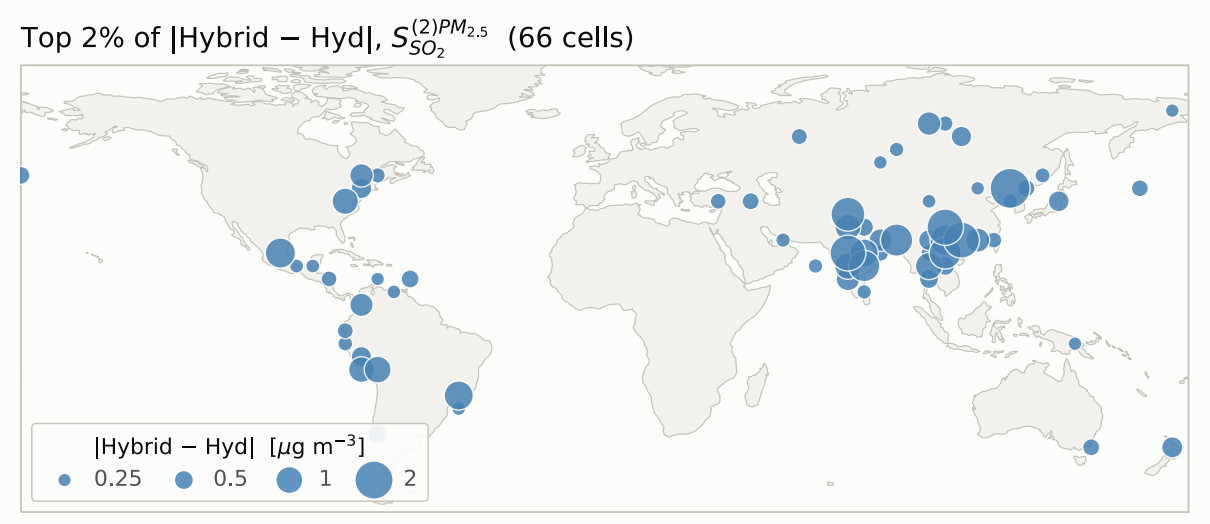

Figure S6. The 2 % of cells with the largest |hybrid − hyd|, sized by that difference of second-order semi-normalized sensitivities of the time-averaged, ground layer $PM_{2.5}$ concentrations with respect to domain-wide, persistent perturbation of SO_2 emissions throughout the 24-hour episode using the hyperdual step method (Hyd) and the hybrid hyperdual-finite difference method (Hybrid) with a 5 % perturbation in each direction.

S3 Simulation Test Scenarios

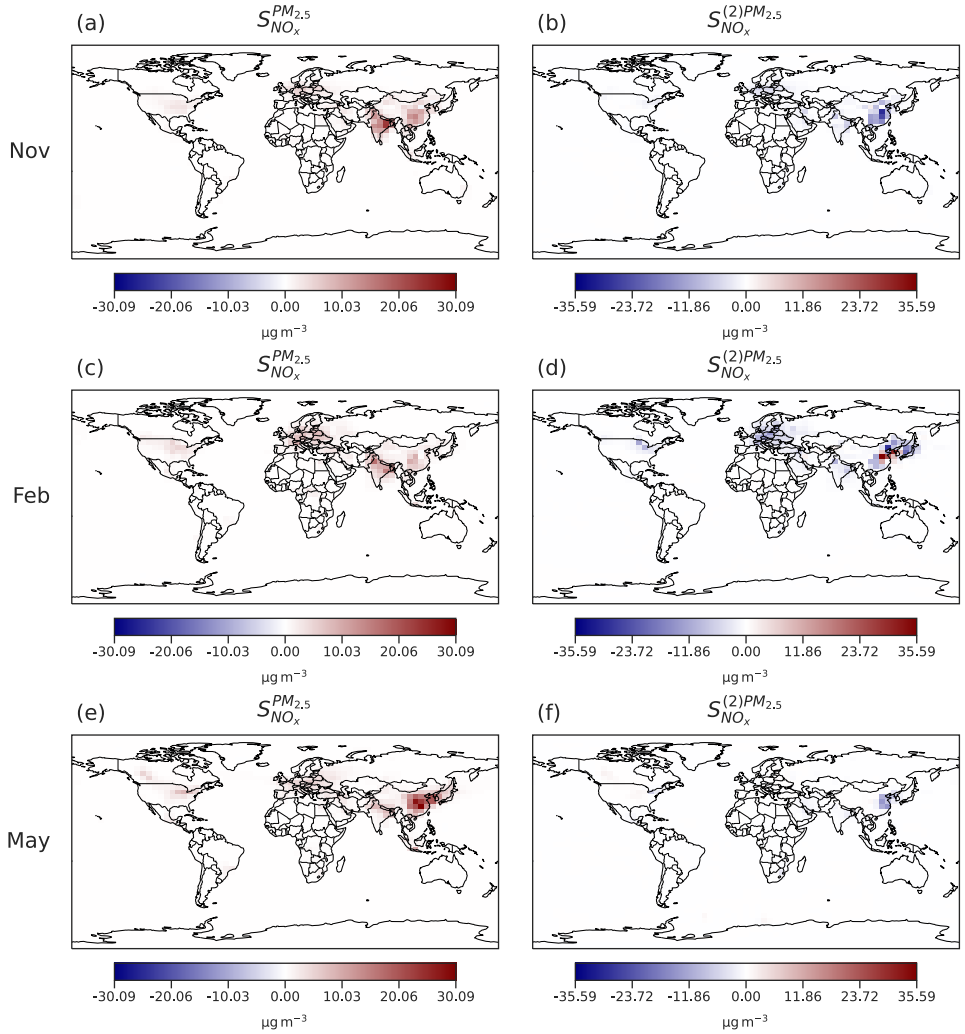

Figure S7. First- and second-order semi-normalised sensitivities of 1-week, time-averaged $PM_{2.5}$ concentrations with respect to domain-wide NO_x emissions on the ground layer for the first week simulation in November (a-b), February (c-d), and May (e-f) of 2019. The first column shows the first-order sensitivities, and the second column shows the second-order sensitivities.

References

Hascoet, L. and Pascual, V.: The Tapenade automatic differentiation tool: Principles, model, and specification, ACM Trans. Math. Softw., 39, Article 20, 10.1145/2450153.2450158, 2013.

Miller, S. J., Makar, P. A., and Lee, C. J.: HETerogeneous vectorized or Parallel (HETPv1.0): an updated inorganic heterogeneous chemistry solver for the metastable-state NH_4^+–Na^+–Ca^{2+}–K^+–Mg^{2+}–SO_4^{2-}–NO_3, Geoscientific Model Development, 17, 2197-2219, 10.5194/gmd-17-2197-2024, 2024.

Press, W. H., Teukolsky, S. A., Vetterling, W. T., and Flannery, B. P.: Numerical Recipes 3rd Edition: The Art of Scientific Computing, Cambridge University Press, 2007.